# Fluorescent Pseudomonas strains from mid-mountain water able to release antioxidant proteins directly into water

Elodie Dussert, Melissa Tourret, Barbara Deracinois, Matthieu Duban, Valérie Leclère, Benoît Cudennec, Rozenn Ravallec, Josette Behra-Miellet

# Title:
# Fluorescent *Pseudomonas* strains from mid-mountain water able to release antioxidant proteins directly into water

**Authors:**

Elodie Dussert[a], Mélissa Tourret[a], Barbara Deracinois[a], Matthieu Duban[a], Valérie Leclère[a], Benoit Cudennec[a], Rozenn Ravallec[a], Josette Behra-Miellet[a*].

**Affiliations:**

[a] *Univ. Lille, INRA, ISA, Univ. Artois, Univ. Côte d'Opale, EA 7394 – ICV – Institut Charles Viollette, F-59000 Lille, F-59655 Villeneuve d'Ascq cedex, France.*

[*] Corresponding author. E-mail address: josette.behra@univ-lille.fr.

[1]**Abbreviations**

[1] (ACN) acetonitrile; (ANI) average nucleotide identity; (BLAST) basic local alignment search tool; (bp) base pairs; (BWA) Burrows-Wheeler aligner; (CFUs) colony forming units; (CHAPS) 3-[(3 cholamidopropyl)dimethylammonio]-1-propanesulfonate; (DNA) deoxyribonucleic acid; (DW) distilled water; (EDTA) ethylenediaminetetraacetic acid; (GC-content) guanine-cytosine content; (HEPES) 4-(2-hydroxyethyl)-1-piperazineethanesulfonic acid; ($HO^{\cdot}$) hydroxyl radical; ($H_2O_2$) hydrogen peroxide; (IC50) half maximal inhibitory concentration; (IEF) isoelectric focusing; (MALDI) matrix assisted laser desorption ionisation; (MLSA) multilocus sequence analysis; (MS) mass spectrometry; (MS/MS) tandem mass spectrometry; (MW) molecular weight; (NAGa) N-acetyl-glucosamine; (NCBI) National center for biotechnology information; ($O_2^{\cdot-}$) superoxide anion; (PACa) phenylacetic acid; (PCA) plate count agar; (PCR) polymerase chain reaction; (pI) isoelectric point; (RAST) rapid annotations using subsystems technology; (ROS) reactive oxygen species; (rRNA) ribosomal ribonucleic acid; (SDS-PAGE) sodium-dodecyl sulfate polyacrylamide gel electrophoresis; (SDW) sterile distilled water; (SOD) superoxide dismutase; (TCS) tetra correlation search; (TFA) trifluoroacetic acid; (TOF/TOF) time-of-flight/time-of-flight; (URE) urease; (X/XO) hypoxanthine/xanthine oxidase; (%id) percentage of identification; (2D-PAGE) two-dimensional polyacrylamide gel electrophoresis.

**Abstract:**
Little is known about fluorescent *Pseudomonas* and investigations are needed to help us better understand how their species work. The aim was here to mimic what naturally occurs in environmental water containing strains isolated from mid-mountain water samples and identified as *Pseudomonas fluorescens* by conventional biochemical techniques. Three strains were cultured before being directly inoculated into distilled water. Surprisingly, the three cell-less extracts obtained after spinning the bacterial suspensions showed strong *in vitro* anti-oxidative effects against superoxide anion and hydroxyl radical but with discrepancies. The extracts obtained were found to contain antioxidant proteins among other stress proteins that were released by viable bacteria. They were identified using tandem/mass spectrometry and showed different profiles in sodium-dodecyl sulfate polyacrylamide gel electrophoresis. Bacterial identification was deepened using 16S ribonucleic acid and genome sequencing analyses to explain the differences observed between strains.

**Keywords:** run-off water, fluorescent *Pseudomonas*, identification, bacterial metabolites, protein, antioxidant.

## 1. Introduction

In this study, we are interested in the possible rejection of antioxidant protein metabolites by fluorescent *Pseudomonas* directly into water susceptible to be dairy ingested. Among the bacteria isolated from mineral waters, only 20% of the strains could be identified by Guillot and Leclerc (Guillot and Leclerc, 1993) and Vachee et al. (Vachee et al., 1997). An important synthesis of the microbiology of natural mineral waters (Leclerc and Moreau, 2002) based on several studies (Bischofberger et al., 1990; Guillot and Leclerc, 1993; Manaia et al., 1990; Vachee et al., 1997) showed that the bacteria most commonly isolated from water belonged to the *Pseudomonas* genus (class of *ɣ-proteobacteria*), with in first position, fluorescent *Pseudomonas* spp., then non-fluorescent *Pseudomonas* spp. The heterogeneity of the *P. fluorescens* group has also been highlighted by Loper et al. (Loper et al., 2012) and genetic variation may underlie differences between strains. They could show discrepancies, for instance in their protein production, in particular that of antioxidant ones. On the other hand, can *P. fluorescens* and its relatives be able to reject antioxidant proteins directly into surrounding water? Indeed, the redox intestine balance plays a judge role in the fight against systemic inflammatory and neurodegenerative diseases (Circu and Aw, 2011) and antioxidant metabolites from natural sources could participate when brought daily in small doses and therefore modulate oxidative stress to optimize therapeutic actions (Chiurchiù et al., 2016). Drinking waters that often contain fluorescent *Pseudomonas* could be antioxidant sources just as those found in the bio vegetal field (Surai et al., 2004) if these bacteria release antioxidant proteins into water. Thus, the goal of this study was to assess the anti-oxidative effects of supernatants obtained after centrifuging simple aqueous bacterial suspensions of three strains identified as *P. fluorescens* using classical phenotypical methods. The cell-less extracts were tested using pharmacological models (without cells) producing reactive oxygen species (ROS). The superoxide anion ($O_2^{\cdot -}$) and hydroxyl ($HO^{\cdot}$) free radicals were measured spectrophotometrically. The proteins released by the three strains were then separated using two-dimensional polyacrylamide gel electrophoresis (2D-PAGE) and identified by mass spectrometry (MS) and/or tandem mass spectrometry (MS/MS) in order to explain the effects observed or any discrepancies in the antioxidant powers of the three supernatants. The aim was also to go further in bacterial identification.

## 2. Materials and methods

## 2.1. Bacterial strains, growth conditions, enumeration, metabolite extraction

### *2.1.1. Bacterial strains, reagents and first phenotypic identification*

*Pseudomonas* strains were isolated from water (of pH 5.5) taken on the granite soil of the Vosges mountains (France) using spraying water on plate count agar (PCA, Biokar Diagnostics, Beauvais, France). Colony forming units (CFUs) were first selected on the ultraviolet ray fluorescence criterion. They were then identified as *P. fluorescens* using phenotypic and biochemical tests such as bacillus morphology with Gram negative staining and oxidase and catalase research, followed by inoculating API® 20 NE (bioMérieux Diagnostics, Marcy-l'Etoile, France). API® 50 CH micro galleries of the same supplier were also inoculated. The three strains to be analysed were named Fl4BN, Fl4BN2 and Fl5BN2.

### *2.1.2. Genotypic characterization of the bacteria*

The second stage of bacterial identification was carried out at the end of the study to explain discrepancies obtained between the strains.

*16S ribosomal ribonucleic acid analysis*

Genotypic characterization of isolates was performed as follows. Total deoxyribonucleic acid (DNA) was extracted using the Wizard Genomic Purification DNA Kit (Promega Corp., Madison, WI, USA). The whole 16S ribosomal ribonucleic acid (rRNA) gene was amplified using primers S1 (5'-AGAGTTTGATCMTGGCTCAG-3') and S2 (5'-GGMTACCTTGTTACGAYTTC-3') (Turner et al., 1999). Polymerase chain reaction (PCR) reaction mixtures containing 5 µl of DNA (40-50 $ng.\mu l^{-1}$), 2.5 µl of each primer (10 µM) and 25 µl of PCR MasterMix (Thermo Fisher Scientific Fermentas, Vilnius, Lituania) in a total volume of 50 µl. PCR thermal cycling was carried out as follows: an initial denaturing step at 95 °C for 3 min, followed by 30 cycles at 95 °C for 30 s, at 55 °C for 30 s and at 72 °C for 2 min, and a final extension step at 72 °C for 7 min. PCR products were purified with the GeneJet PCR purification kit (Thermo, France). Then, purified PCRs were sequenced by the Custom Sequencing Service of Eurofins Genomics (Ebersberg, Germany) using cycle sequencing technology on ABI PRISM 3730XL. Two sequencing reactions generating both forward and reverse sequences were required to cover the length of the 16S rRNA gene. The forward and reverse sequences were aligned so that identical sequences (100% identity) were with a minimum of 50 base pairs (bp) and were assembled to obtain the full contiguous sequence. These sequences were then compared with GenBank databases using basic local alignment search tool (BLAST) software provided online by the National center for biotechnology information (NCBI, Bethesda, MD, USA).

*Whole genome analysis*

The detailed method is presented in Data in Brief. Briefly, after extracting and sequencing total DNA, the closest existing reference genome was determined using Kraken (Wood and Salzberg, 2014), and data quality was assessed by mapping the reads using the Burrows-Wheeler aligner (BWA) MEM algorithm (http://bio-bwa.sourceforge.net). The reads were assembled and gene function prediction was performed by the rapid annotations using subsystems technology (RAST) server (http://rast.nmpdr.org) (Aziz et al., 2008) followed by an annotation using the SEED database (Disz et al., 2010). The alignments of the bacterial draft genomes with the complete genomes of the nearest species determined by average nucleotide identity (JSpecies) (*Pseudomonas* sp. Lz4W and *P. fragi* P121 for Fl4BN2 and *Pseudomonas protegens* CHA0 for Fl4BN1 and Fl5BN2) were also performed using the Progressive MAUVE algorithm (Darling et al., 2010).

*Average nucleotide identity (ANI) and tetra-nucleotide signatures analyses*

The detailed methods are available in Data in Brief. Bacteria draft genomes were compared using the JSpecies software (Ribocon GmbH; http://jspecies.ribohost.com/jspeciesws/) with indices based on the analysis of whole-genome sequences. Thus, tetra correlation search (TCS), ANIb (based on the BLAST algorithm) and ANIm (based on the MUMmer ultra-rapid aligning tool) were performed (Camacho et al., 2009; Goris et al., 2007; Richter et al., 2016; Teeling et al., 2004).

*2.1.3. Growth conditions, enumeration and metabolite extraction*

After preliminary growth, bacteria were aerobically cultured at 25 °C for 5 days in broth medium prepared with tryptone (2.5 $g.L^{-1}$) (Euromedex®, Souffelweyersheim, France) and yeast extract (1.25 $g.L^{-1}$) (Conda Laboratories, Madrid, Spain) in distilled water (DW). The broths containing the strains were transferred into pre-sterile centrifuge tubes to be then centrifuged at 10,000 g for 13 min at 4 °C (Sorvall Evolution RC Centrifuge, Thermo Fisher Scientific, Asheville, NC, USA). The supernatants were removed and the pellet cells were washed and diluted in Ringer ¼ medium (Oxoid, Hampshire, England). To assess the viability and/or growth of bacteria after culture, the spreading of 100 µl of the suitably diluted cells was done on PCA surface before aerobic incubation at room temperature. After centrifugation, followed by two successive washes in sterile DW (SDW), the pellets of the pure *P. fluorescens* strains -Fl4BN1, Fl4BN2 and Fl5BN2- were weighted, before being placed in agitation in SDW (250 mg of moist bacteria.$ml^{-1}$) overnight at 4 °C. Counts were also performed before (named Cb) and after (named Ca) agitating in order to assess the viability of the microorganisms by spreading suitable suspension dilutions onto PCA as above described. The suspensions were then centrifuged at 20,000 g for 1 hour at 4 °C (Centrifuge 5417R, Eppendorf, Hamburg, Germany). Supernatants without cells were collected and stored at -32 °C. They constituted the bacterial extracts named E-Fl4BN1, E-Fl4BN2, and E-Fl5BN2. They were supposed to contain metabolites, especially protein metabolites released by each of the microorganisms.

2.2. Pharmacological in vitro assays

*2.2.1. Bacterial extract concentrations and reagents*

The extracts were tested at the increasing concentrations ranged from 5 to 100 µl.$ml^{-1}$ of final reaction mixtures. All reagents were purchased from Sigma-Aldrich (Saint-Quentin Fallavier, France).

*2.2.2. In vitro measurement of the anti-oxidative effect of the bacterial extracts on superoxide anion*

The hypoxanthine/xanthine oxidase system (X/XO) was used to produce superoxide anion *in vitro*. The $O_2^{\cdot-}$ inhibition by E-Fl4BN1, E-Fl4BN2, or E-Fl5BN2 was quantified according to Aruoma et al. (Aruoma et al., 1989) using the reduction of ferricytochrome C. The supernatants were poured at each concentration into a final volume of 1 ml containing 0.1 mM xanthine, 1 mM ethylenediaminetetraacetic acid (EDTA), 0.017 mM ferricytochrome C in Hank's/4-(2-hydroxyethyl)-1-piperazineethanesulfonic acid (HEPES) buffer pH 7.42. Xanthine oxidase was added and the reaction medium was incubated at room temperature for 5 min before measuring the ferricytochrome C reduction at the wavelength of 550 nm using a Multiskan FC spectrophotometer (Thermo Fisher Scientific Instruments Co, Shanghai, China) against blank controls containing all the reagents except X/XO. Positive inhibition controls (0.3 mM cysteine) were also assessed in each series of tests. Finally, the ferricytochrome C

extinction coefficient (ε550 nm = $2.11 \times 10^{-8}$ $M^{-1}cm^{-1}$) was used to convert absorbances to nanomoles of superoxide anion.

*2.2.3. In vitro measurement of the anti-oxidative effect of the bacterial extracts on hydroxyl radical*

The inhibition of $HO^{\cdot}$ by E-Fl4BN1, E-Fl4BN2, and E-Fl5BN2 was evaluated according to a method adapted from that described by Halliwell B., Gutteridge J.M.C. and Aruoma O.I. (Halliwell et al., 1987). $HO^{\cdot}$ was produced from 9 to 15 $nmol.ml^{-1}$ of hydrogen peroxide ($H_2O_2$) in each tube in 20 mM $KH_2PO_4$ medium at pH 7.4 in the presence of $FeCl_3$ 100 µM, 104 $\mu mol.L^{-1}$ EDTA and 100 $\mu mol.L^{-1}$ ascorbic acid to generate $HO^{\cdot}$ according to Fenton's reaction. This radical was then inhibited by the increasing E-Fl4BN1, E-Fl4BN2, and E-Fl5BN2 concentrations before adding 3 mM deoxyribose and incubating the reaction medium at 37 °C for 30 min. After boiling for 20 min, the malondialdehyde resulting from the deoxyribose degradation by the rest of $HO^{\cdot}$ (non-inhibited by the bacterial extracts) in the presence of 14 mM thiobarbituric acid and 147 mM trichloroacetic acid was quantified by spectrophotometry at the wavelength of 532 nm ($\lambda_{532\ nm}$). In these assays, absorbance was also red against blank control tubes containing all reagents except $H_2O_2$. Positive inhibition controls (0.3 mM cysteine) were also assessed in each series of tests.

2.3. Proteomic analysis

*2.3.1. Two-dimensional polyacrylamide gel electrophoresis*

The proteins contained in E-Fl4BN1, E-Fl4BN2, and E-Fl5BN2 were separated by 2D-PAGE as previously described (Hochart-Behra et al., 2014). Bacterial extracts (all at a volume equivalent to 500 µg-proteins released by FL4BN1 or FL4BN2 or FL5BN2) were desalted at a cut-off of 10-kDa in Microcon® filters (Millipore, Bedford, USA), re-solubilized in SDW and lyophilized (LP3, Jouan, Saint Herblain, France). Protein rehydration was performed in 7 mM urea (Sigma, Saint-Quentin Fallavier, France), 2 M thiourea (Sigma), 65 mM 3-[(3-cholamidopropyl)dimethylammonio]-1-propanesulfonate (CHAPS), 0.4% (vol/vol) Triton X 100, a hint of bromophenol blue (Sigma) and 0.625% (vol/vol) pH 3–10 Biolyte® (Bio-Rad, Marnes la Coquette, France). Isoelectric focusing (IEF) was done by loading the proteins onto precast immobilized pH 3–10 gradient ReadyStrip® (17 cm, Bio-Rad) using the Bio-Rad Protean IEF cell system.

Sodium-dodecyl sulfate polyacrylamide gel electrophoresis (SDS-PAGE) experiments were then performed under non-denaturing conditions (such as a low concentration of SDS, absence of reducing and/or alkylating agents). SDS-PAGE gels were obtained with 4–20% acrylamide gradient using an acrylamide/bisacrylamide (29:1) solution (Bio-Rad) containing only 0.1% SDS. After rehydration in migration buffer (Tris, glycine, SDS), the strips were put at the top of the second-dimension gel in a 10 $g.L^{-1}$ agarose solution in migration buffer (Serva, Heidelberg, Germany). Precision Plus Protein Standards® solution (Bio-Rad) was also loaded next to the vertical migration of bacterial extract proteins. Proteins were first fixed on the gels, washed and colored by colloidal Coomassie blue staining (G250 brilliant blue, Sigma). Gel images were then acquired as previously described using a GS800 densitometer (Bio-Rad) and PDQuest software (Bio-Rad). Interesting protein spots were excised (Hochart-Behra et al., 2008) in order to perform protein identification by peptide mass or fragment fingerprinting.

*2.3.2. Protein identification by MS and/or MS/MS*

Protein spots of interest were in-gel-trypsin-digested after several treatments (with reduction and alkylation of disulfide bonds) described by Hochart-Behra et al. (Hochart-Behra et al.,

2008). Peptides were finally extracted from protein bands with 0.1% trifluoroacetic acid (TFA) in acetonitrile (ACN)-DW (vol/vol) solution. Those supernatants were dried and re-suspended in 0.1% TFA (vol/vol) in DW solution before being concentrated and desalted by the same solution on a ZipTip C18 ® column (Millipore).
Mass analysis was performed using an Autoflex Speed$^{TM}$ matrix assisted laser desorption ionisation (MALDI) time-of-flight/time-of-flight (TOF/TOF) mass spectrometer (Bruker, Bremen, Germany) as previously described by Shevchenko et al. (Shevchenko et al., 1996) and Ceugniez et al. (Ceugniez et al., 2017). The detail of the identification method is provided in Data in Brief as far as deposition of the peptides eluted on the target plate, molecular mass measurements, and database searches are concerned.

2.4. Statistical analysis

The bacterial population viability was assessed using comparison between the counts obtained before and after the extraction process. Non-parametric sign-test was used (Wilcoxon's matched-pair test, Graphpad Prism 7.00 software, La Jo la, USA) at the 5% level (n = 6 independent experiments). For pharmacological *in vitro* assays, the data was analysed from six independent assays using analysis of variances in case of data normality and variance homogeneity both checked using Graphpad Prism 7.00 software and AnaStat Scope ARL software for Levene's test. In the other cases, Kruskal & Wallis test was used at the 5% level ($p = 0.05$) (Graphpad Prism 7.00 software). Results were presented as box-plots where the extremities of the lowest and the highest bars represent the 10th and 90th percentiles of percentages for each extract concentration. The 25th, 50th and 75th percentiles correspond to the inferior, interior and superior horizontal bars of the boxes constructed for each of the extract concentrations.

## 3. Results

3.1. Bacteria identification through classical phenotypic methods

Several techniques were used in order to identify the bacterial strains of interest (Fl4BN1, Fl4BN2 and Fl5BN2). First, a classical phenotypic identification was carried out (based on API® 20 NE and API® 50 CH galleries). The biochemical profiles found for the three strains using API® 20 NE identified these fluorescent strains as *P. fluorescens*. The percentage of identification (% id) reached 97.2% for Fl4BN1 (T = 0.79; phenylacetic acid or PACa 16%), 99.9% for Fl4BN2 (T = 0.67; urease or URE 1%), and for Fl5BN2, % id was found at 99.3% for numerical profile 0156457 (T = 0.66; N-acetyl-glucosamine or NAGa 85%; PACa 16%) and at 97.2% for numerical profile 0156557 (T = 0.79; PACa 16%). More information was obtained for all strains with their biochemical profiles using API® 50 CH (Data in Brief Table 1). Thus Fl4BN1 and Fl5BN2 profiles were very similar. Both strains were able to assimilate the same substrates to varying degrees, particularly D-mannitol, potassium gluconate and potassium 2-ketogluconate. The Fl4BN2 pattern differed slightly by the oxidation of D-fucose or glycerol or D-mannose and by the assimilation of D and L-arabinose, D-xylose, D-galactose, L-fucose.

3.2. Second stage of genotypic bacterial identification

The second identification approach consisting in analyzing strain 16S RNA confirmed their probable belonging to the genus *Pseudomonas*.
To determine which bacterial species the strains belong to, sequencing of the entire genome was performed at MicrobesNG. For Fl4BN1, the draft genome of 7333320 bp included 92 contigs with a GC-content (guanine-cytosine content) of 61.51% and a N50 contig size of 196900 bp was obtained. Gene function prediction and annotation result in 71 RNAs and

6601 coding sequences. For Fl4BN2, the draft genome of 5294323 bp included 181 contigs with a GC-content of 58.85%, a N50 contig size of 361713 bp, 84 RNAs and 4622 coding sequences were obtained. For Fl5BN2, the draft genome of 7205711 bp included 59 contigs with a GC-content of 61.55%, a N50 contig size of 250648 bp, 73 RNAs and 6442 coding sequences were obtained.
TCS feature in JSpecies software allows to search any draft genome against entire genomes reference database GenomesDB and provides an insight into the relationships among organisms. By this way, the draft genomes of Fl4BN1 and Fl5BN2 were found very close to *Pseudomonas batumici* UCM B-321 strain and *Pseudomonas protegens* Cab57 strain, with Z-scores higher than 0.989 for Fl4BN1 and Fl5BN2 (Data in Brief Table 2) while the Fl4BN2 scores seemed more in favor of *Pseudomonas fragi* P121 and *Pseudomonas* sp. Lz4W as shown in Data in Brief Table 2. Pairwise genome comparison was performed using JSpecies to measure the probability that genomes belonged to the same species with their ANI. ANI analyses of genome sequences seemed to support these results (Data in Brief Tables 3 and 4). As shown in Data in Brief Figure 1, alignments performed using MAUVE illustrated ANI results.

### 3.3. Bacteria viability during extraction

Bacteria's ability to grow again after the extraction process was assessed by counting the CFUs before (Cb) and after (Ca) incubation overnight at 4 °C in SDW. Mean counts of CFUs from 6 independent experiments were similar for the three strains with small variations between Cb and Ca whose values were $1.39 \times 10^{11}$ and $1.02 \times 10^{11}$, $1.37 \times 10^{10}$ and $2.25 \times 10^{10}$, $9.51 \times 10^{10}$ and $7.79 \times 10^{10}$, for Fl4BN1, Fl4BN2 and Fl5BN2, respectively. No significant differences were found between Cb and Ca using the non-parametric statistical Wilcoxon's matched-pairs test at the $p = 0.05$ level for each strains, since the exacts $p$ values were 0.6875, 0.6250 and 0.1563 for Fl4BN1, Fl4BN2 and Fl5BN2, respectively.

### 3.4. In vitro effects of the extracts on superoxide anion and hydroxyl radical

#### *3.4.1. Superoxide anion inhibition*

As shown in Fig. 1, each cysteine control could be validated and the three strain extracts showed *in vitro* a statistically significant inhibition of superoxide anion using one-way ANOVA ($p < 0.0001$ with the overall Fisher's test at the $p = 0.05$ level for the three bacterial extracts and 6 independent experiments). For E-Fl4BN1, this effect compared with that of the control without extract was statistically significant from 25 µl of extract per ml ($p = 0.0441$ using the Tukey's multiple comparison test at the $p = 0.05$ level) and very different for the 100 µl concentration of extract per ml ($p < 0.0001$). The mean concentration of superoxide anion decreased from 8.40 ± 0.77 nmol.ml$^{-1}$ for the control to 3.36 ± 1.66 nmol.ml$^{-1}$ at 100 µl of E-Fl4BN1.ml$^{-1}$. The inhibition of $O_2^{\cdot -}$ by E-Fl4BN2 was also statistically significant from 25 µl of E-Fl4BN2 per ml ($p = 0.0278$ using the Tukey's test above mentioned). The mean difference between the superoxide anion concentration obtained for the controls without E-Fl4BN2 and that observed for 100 µl of E-Fl4BN2 per ml reached about 3.1 nmol of $O_2^{\cdot -}$.ml$^{-1}$, as this superoxide anion concentration decreased from 9.16 ± 0.58 to 6.09 ± 0.66 nmol.ml$^{-1}$ ($p < 0.0001$). As for the mean inhibition of $O_2^{\cdot -}$ by E-Fl5BN2, it reached about 4.2 nmol of superoxide anion.ml$^{-1}$ at the highest concentration of bacterial extract tested (100 µl.ml$^{-1}$), as the mean $O_2^{\cdot -}$ concentration diminished from about 9.00 ± 0.67 to 4.75 ± 0.76 nmol.ml$^{-1}$ between the control without extract and the tubes containing 100 µl of E-Fl5BN2.ml$^{-1}$. For the latter, the inhibition effect on $O_2^{\cdot -}$ was significant from the E-Fl5BN2 concentration of 10 µl.ml$^{-1}$ ($p = 0.035$ using the Tukey's multiple comparison test). Half maximal inhibitory

concentration (IC50) could be calculated for E-Fl4BN1 and the concentration range tested (67 µl.ml$^{-1}$).

*3.4.2. Hydroxyl radical inhibition*

Six independent experiments were carried out. The model was also validated by the positive control of HO$^{\cdot}$ inhibition (0.3 mM cysteine). As shown in Fig. 2, E-Fl4BN1 and E-Fl5BN2 showed high inhibitory effects against HO$^{\cdot}$ as this ROS was almost completely scavenged by 100 µl of bacterial extracts per ml of reaction medium. This inhibition was statistically significant ($p < 0.0001$ using the Kruskal-Wallis test) from the E-Fl4BN1 and E-Fl5BN2 concentration of 50 µl.ml$^{-1}$ ($p = 0.0082$ and 0.0024, respectively) using the Dunn's multiple comparison test. The decreases of the mean HO$^{\cdot}$ concentration were very pronounced for both strain extracts at 100 µl.ml$^{-1}$ compared with the controls without extracts (from 10.94 ± 0.64 to 0.43 ± 0.63 for E-Fl4BN1 and from 12.53 ± 1.24 to 0.12 ± 0.15 nmol of HO$^{\cdot}$.ml$^{-1}$ for E-Fl5BN2). A lesser inhibitory effect of E-Fl4BN2 was also shown against hydroxyl radical which remained significant from the concentration of 50 µl of extract.ml$^{-1}$ using ANOVA (overall Fisher's test, $p < 0.0001$; Tukey's multiple comparison test, $p = 0.0212$). For this latter extract, the hydroxyl radical concentration decreased from 12.91 ± 1.18 nmol of HO$^{\cdot}$.ml$^{-1}$ (observed with the control without extract) to 8.75 ± 1.33 nmol of HO$^{\cdot}$.ml$^{-1}$ (shown with E-Fl4BN2 at 100 µl.ml$^{-1}$). The IC50 possible to be calculated in the concentration range were 9 and 11 µl.ml$^{-1}$ for E-Fl4BN1and E-Fl5BN2, respectively.

3.5. Identification of the proteins separated by 2D-PAGE

The protein 2D-profiles were obtained for E-Fl4BN1, E-Fl4BN2 and E-Fl5BN2 (Fig. 3A, 3B, 3C, respectively). E-Fl4BN1 and E-Fl5BN2 protein profiles showed similarities but seemed to differ from that of E-Fl4BN2 proteins.

Stress proteins were identified (14 spots corresponding to 12 different proteins for Fl4BN1 strain, 18 spots corresponding to 7 different proteins for Fl4BN2 strain, and 19 spots corresponding to 11 different proteins for Fl5BN2 strain; MS and MS/MS combined) in the native gels that were classified in Fig. 3 in three types and whose identification was specified in Data in Brief Table 5 (MS data for the three strains) and in tables 6-7, 8-9, 10-11 (MS/MS data for the extracts from Fl4BN1, Fl4BN2 and Fl5BN2, respectively). Proteins relative to oxidative stress were first found such as superoxide dismutase (SOD) (spots Fl4BN1-o4 and Fl5BN2-o5), dihydrolipoyl dehydrogenase (spots Fl4BN1-o1, Fl5BN2-o1-o4), glutaredoxin (spot Fl4BN2-o1), peroxiredoxin (spot Fl4BN1-o2) and ketol-acid reductoisomerase (Fl4BN1-o3). These proteins represent 28.6%, 5.6% and 26.3% of the proteins identified for Fl4BN1, Fl4BN2 and Fl5BN2, respectively. Chaperonin proteins were also identified such as chaperone protein DnaK (spots Fl4BN1-c1, Fl4BN2-c1-6, Fl5BN2-c6 and c7), chaperone protein HtpG (spots Fl4BN1-c2, Fl4BN2-c7 and c8, Fl5BN2-c1), 60 kDa chaperonin or GroEL (spots Fl4BN1-c3, and c6, Fl5BN2-c2 and c3), trigger factor (spots Fl4BN1-c4, Fl4BN2-c9-c11, Fl5BN2-c4), nucleotide exchange factor GrpE (spots Fl4BN1-c7, Fl4BN2-c12 and c13), peptidyl-prolyl-cis-trans isomerase (spots Fl4BN2-c14, Fl5BN2-c8 and c9) and finally molecular chaperone SurA (spots Fl4BN1-c5, Fl5BN2-c5). Chaperonin represent 50%, 77.7% and 47.4% of the proteins identified for Fl4BN1, Fl4BN2 and Fl5BN2, respectively. Other proteins involved in stress response were detected such as the tail-specific protease also called peptidase S41 or serine peptidase (spots Fl4BN1-p1 and Fl5BN2-p1), cold shock proteins (spots Fl4BN1-p2 and p3, Fl4BN2-p1-p3, Fl5BN2-p4 and p5), DNA-binding protein HU beta subunit also named nucleoid protein HU or transcriptional regulator (Fl5BN2-p2 and p3), representing 21.4%, 16.7% and 26.3% of the proteins identified for Fl4BN1, Fl4BN2 and Fl5BN2, respectively. Other proteins that were involved in the biosynthesis and /or metabolism of carbohydrates, amino acids, proteins related to transport or energy or protein

binding, or ribosomal proteins, asparaginase and ferric uptake regulation protein were also identified in gels.

## 4. Discussion

Our study focuses on spring water bacteria, which have been identified by conventional phenotypic techniques as *P. fluorescens*. The goal was in one hand to study the ability of these strains to produce antioxidant metabolites in acidic (pH 5.5) run-off waters that are known as exempt of contaminants such as pesticides or coliforms and very low in salts and on the other hand, to find out if these cell-less extracts had antioxidant power. For this reason, their activities on $O_2^{\cdot -}$ and $HO^{\cdot}$ were studied because they are essential radicals produced in case of inflammation in humans. Our results showed that the three strain extracts significantly decreased $O_2^{\cdot -}$ production, depending on their concentration. The effect was more pronounced for Fl4BN1 and Fl5BN2 compared with Fl4BN2 as shown in Fig. 1. The strains were therefore capable of releasing metabolites that had antioxidant effects against these ROS. An inhibition by the three extracts was also found against $HO^{\cdot}$, a very reactive and deleterious species towards tissues and cells. Fl4BN2 cell-free extract was another time less potent as IC50 could not be calculated for this extract (Fig. 2). Therefore, these functional differences between the three strains led to perform 2D-PAGE to characterize the proteins released into water. Protein associations (dimers or more associated protein monomers) could be preserved in non-denaturing gels and detected by MS analysis. Breaking in protein fragments could however also occur. Bacterial extracts were desalted at a cut-off of 10-kDa explaining why the protein molecular weight (MW) analyzed were higher than 9-10 kDa. The majority of the spots have isoelectric point (pI) ranging from 4.5 to 7. For both Fl4BN1 and Fl5BN2 strains, fairly similar protein profiles were found, unlike the Fl4BN2 protein profile. For example, intense spots of 60 kDa-chaperonin were found in the gel performed with Fl4BN1 and Fl5BN2 extracts as shown in Fig. 3A, 3C, but not for Fl4BN2 (Fig. 3B). Only a few proteins seemed to be constantly found in gels for all strains studied, that ranged from 10 and 15 kDa and that were identified as cold-shock proteins according their psychrophilic behavior in mountain water. These data suggest that Fl4BN1 and Fl5BN2 could be very close fluorescent *Pseudomonas* strains, unlike FL4BN2 in the same genus.

Proteins counteracting oxidative stress and/or ensuring redox balance were found in the three extracts but with notable differences. SOD and dihydrolipoyl dehydrogenase were both found for Fl4BN1 and Fl5BN2. SOD explains the inhibitory effect found against superoxide anion and dihydrolipoyl dehydrogenase could participate in the hydroxyl radical detoxification. Dihydrolipoyl dehydrogenase (also called dihydrolipoamide dehydrogenase) seems to be detected, in its monomeric form (Fl5BN2-o3, Fl5BN2-o4): these two spots have same MW but different isoelectric point values, which can indicate post-translational changes, such as successive phosphorylations (Rosen et al., 2004) and in its dimeric form: Fl4BN1-o1 spot matches the dihydrolipoyl dehydrogenase protein with a theoretical MW at 49.8 kDa whereas the experimental MW reached 100 kDa in the gel. This protein is known to exist as an homodimer (Yang et al., 2019), but also as a monomer (Babady et al., 2007). In our study, dihydrolipoyl dehydrogenase would also be detected in its trimeric version (Fl5BN2-o2 at around 150 kDa in gel) or quadrimeric form (Fl5BN2-o1 at around 200 kDa in gel) which have not been described in other studies. The Fl4BN1 strain released proteins into water that were not found for both other bacteria, such as peroxiredoxin (Fl4BN1-o2) with a theoretical MW at 21.7 kDa whereas this protein MW was found at around 40 kDa in gel. Thus, we can suggest it is a peroxiredoxin dimer and this is consistent with other (Noguera-Mazon et al., 2006). Among the chaperonin proteins, protein GrpE was found for Fl4BN1 and Fl4BN2, but not for Fl5BN2. Chaperones such as the major ubiquitous DnaK and GroEL, have crucial roles, assisting proteins in their folding and assembling, in preventing their misfolding and

aggregation under stress conditions (Hartl et al., 2011), and in their transport. DnaK formed monomers, dimers, and oligomers of higher MW (Schönfeld et al., 1995). The spot Fl4BN1-c8 concerned a nucleotide exchange factor GrpE with a MW of about 25 kDa in accordance with the monomeric form, knowing that GrpE could also exist in a dimeric or an oligomeric form (Wu et al., 1996). Zylicz and his team described GrpE monomers (Zylicz et al., 1987). An in-depth review of the proteins identification obtained by the technique of peptide mapping by mass through the "Mascot" search algorithm and by the technique of peptide mapping by mass through the "PEAKS studio" search algorithm (Data in Brief Tables 4 to 11) showed that many species stood out in the identifications, probably because the proteins had conserved sequences. In order to explain the differences observed between strains, analysis was performed on the three genomes. As in prior studies, 16S RNA sequences alone cannot distinguish between *Pseudomonas* species (Garrido-Sanz et al., 2016; Gomila et al., 2015). Thus, our study focused on TCS and ANI indices to thorough strain identification, because both techniques are based on the analysis of whole-genome sequences, compared with multilocus sequence analysis (MLSA) studying a small number of genes (Data in Brief Tables 2-4). The study of Gomila et al. showed that tetra-nucleotide signature was useful for discriminating *Pseudomonas* from other genera, whereas ANIb separated strains of different species and showed the strongest correlation with MLSA (Gomila et al., 2015). Indeed, TCS has confirmed the belonging of the three strains to the *Pseudomonas* genus. The ANI calculated for Fl4BN1 and Fl5BN2 showed that both strains belonged with a value above the 95%-threshold to the same species as shown in Data in Brief Tables 3 and 4, whereas Fl4BN2 was found close to *Pseudomonas fragi* and *Pseudomonas* sp. Lz4W with a pairwise ANI value higher than the threshold demarking species delineation. The draft genome alignments presented in Data in Brief Figure 1 showed major differences between the strains and their similarities with other species than *P. fluorescens*. However the latter appears to break out into several groups showing its great diversity (Garrido-Sanz et al., 2017) and our three strains could also illustrate their belonging to different of these groups. Further investigations are needed and planned based on the complete decryption of bacterial genomes.
Above all, we retain from this study the surprising ability of strains isolated from mountain water samples to be viable and to release proteins directly into DW, without adding any detergent. Indeed, previous studies have shown the need to use a mild non-ionic detergent to produce stress proteins by bacteria such as *Bacteroides thetaiotaomicron* (Hochart-Behra et al., 2014).

## 5. Conclusion

Thus, this data illustrates the diversity of fluorescent *Pseudomonas* and shows that non-pathogenic bacteria of spring water daily ingested by local residents could release metabolites of interest regarding redox human homeostasis. However, to prove whether these bacterial metabolites are really beneficial to humans, further investigations need to be considered such as checking the antioxidant and safety effects of the extracts, first in cell models, then in animals.

## Declaration of interest

All authors declare that there is no potential or actual conflict of interest in relation to this research study.

## Acknowledgments

The authors thank all the bodies that contributed to the funding of this study (listed above). They thank also D. HUGES for his contribution to English language.

**Funding statement**

The REALCAT platform is benefiting from a state subsidy administrated by the French National Research Agency (ANR) within the frame of the 'future Investments' program (PIA), with the contractual reference 'ANR-11-EQPX-0037'. The European Union, through the ERDF funding administered by the Hauts-de-France Region, has co-financed the platform. Centrale Lille, the CNRS, and Lille University as well as the Centrale Initiative Foundation, are thanked for their financial contribution to the acquisition and implementation of the equipment of the REALCAT platform. The Hauts-de-France Region attributed the thesis Region Contract N°17007747 to Elodie Dussert for her studies that were also performed thanks to the 'Contrats de Plan ETAT-REGION' CPER PO 2015-2020 ALIBIOTECH.

**References**

Aruoma, O.I., Halliwell, B., Hoey, B.M., Butler, J., 1989. The antioxidant action of N-acetylcysteine: its reaction with hydrogen peroxide, hydroxyl radical, superoxide, and hypochlorous acid. Free Radic. Biol. Med. 6, 593–597. https://doi.org/10.1016/0891-5849(89)90066-x

Aziz, R.K., Bartels, D., Best, A.A., DeJongh, M., Disz, T., Edwards, R.A., Formsma, K., Gerdes, S., Glass, E.M., Kubal, M., Meyer, F., Olsen, G.J., Olson, R., Osterman, A.L., Overbeek, R.A., McNeil, L.K., Paarmann, D., Paczian, T., Parrello, B., Pusch, G.D., Reich, C., Stevens, R., Vassieva, O., Vonstein, V., Wilke, A., Zagnitko, O., 2008. The RAST Server: rapid annotations using subsystems technology. BMC Genomics 9, 75. https://doi.org/10.1186/1471-2164-9-75

Babady, N.E., Pang, Y.-P., Elpeleg, O., Isaya, G., 2007. Cryptic proteolytic activity of dihydrolipoamide dehydrogenase. Proc. Natl. Acad. Sci. U. S. A. 104, 6158–6163. https://doi.org/10.1073/pnas.0610618104

Bischofberger, T., Cha, S. k., Schmitt, R., König, B., Schmift-Lorenz, W., 1990. The bacterial flora of non-carbonated, natural mineral water from the springs to reservoir and glass and plastic bottles. Int. J. Food Microbiol. 11, 51–71. https://doi.org/10.1016/0168-1605(90)90039-8

Camacho, C., Coulouris, G., Avagyan, V., Ma, N., Papadopoulos, J., Bealer, K., Madden, T.L., 2009. BLAST+: architecture and applications. BMC Bioinformatics 10, 421. https://doi.org/10.1186/1471-2105-10-421

Ceugniez, A., Tourret, M., Dussert, E., Coucheney, F., Deracinois, B., Jacques, P., Flahaut, C., Heuson, E., Drider, D., Behra-Miellet, J., 2017. Interactions between *Kluyveromyces marxianus* from cheese origin and the intestinal symbiont *Bacteroides thetaiotaomicron*: Impressive antioxidative effects. LWT - Food Sci. Technol. 81, 281–290. https://doi.org/10.1016/j.lwt.2017.03.056

Chiurchiù, V., Orlacchio, A., Maccarrone, M., 2016. Is modulation of oxidative stress an answer? The state of the art of redox therapeutic actions in neurodegenerative diseases. Oxidative Med. Cell. Longev. Vol 2016 2016 2016, 11. https://doi.org/10.1155/2016/7909380

Circu, M.L., Aw, T.Y., 2011. Redox biology of the intestine. Free Radic. Res. 45, 1245–1266. https://doi.org/10.3109/10715762.2011.611509

Darling, A.E., Mau, B., Perna, N.T., 2010. progressiveMauve: multiple genome alignment with gene gain, loss and rearrangement. PloS One 5, e11147. https://doi.org/10.1371/journal.pone.0011147

Disz, T., Akhter, S., Cuevas, D., Olson, R., Overbeek, R., Vonstein, V., Stevens, R., Edwards, R.A., 2010. Accessing the SEED genome databases via Web services API: tools for programmers. BMC Bioinformatics 11, 319. https://doi.org/10.1186/1471-2105-11-319

Garrido-Sanz, D., Arrebola, E., Martínez-Granero, F., García-Méndez, S., Muriel, C., Blanco-Romero, E., Martín, M., Rivilla, R., Redondo-Nieto, M., 2017. Classification of isolates from

the *Pseudomonas fluorescens* complex into phylogenomic groups based in group-specific markers. Front. Microbiol. 8, 413. https://doi.org/10.3389/fmicb.2017.00413
Garrido-Sanz, D., Meier-Kolthoff, J.P., Göker, M., Martín, M., Rivilla, R., Redondo-Nieto, M., 2016. Genomic and genetic diversity within the *Pseudomonas fluorescens* complex. PloS One 11, e0150183. https://doi.org/10.1371/journal.pone.0150183
Gomila, M., Peña, A., Mulet, M., Lalucat, J., García-Valdés, E., 2015. Phylogenomics and systematics in *Pseudomonas*. Front. Microbiol. 6, 214. https://doi.org/10.3389/fmicb.2015.00214
Goris, J., Konstantinidis, K.T., Klappenbach, J.A., Coenye, T., Vandamme, P., Tiedje, J.M., 2007. DNA-DNA hybridization values and their relationship to whole-genome sequence similarities. Int. J. Syst. Evol. Microbiol. 57, 81–91. https://doi.org/10.1099/ijs.0.64483-0
Guillot, E., Leclerc, H., 1993. Bacterial flora in natural mineral waters: characterization by ribosomal ribonucleic acid gene restriction patterns. Syst. Appl. Microbiol. 16, 483–493. https://doi.org/10.1016/S0723-2020(11)80284-5
Halliwell, B., Gutteridge, J.M., Aruoma, O.I., 1987. The deoxyribose method: a simple "test-tube" assay for determination of rate constants for reactions of hydroxyl radicals. Anal. Biochem. 165, 215–219. https://doi.org/10.1016/0003-2697(87)90222-3
Hartl, F.U., Bracher, A., Hayer-Hartl, M., 2011. Molecular chaperones in protein folding and proteostasis. Nature 475, 324–332. https://doi.org/10.1038/nature10317
Hochart-Behra, A.-C., Behra-Miellet, J., Sam, J., Drobecq, H., Gressier, B., Luyckx, M., Dine, T., Brunet, C., Dubreuil, L., 2008. Antioxidative effect of *Bacteroides thetaiotaomicron* extracts: superoxide dismutase identification. Anal. Bioanal. Chem. 391, 415–423. https://doi.org/10.1007/s00216-008-1993-0
Hochart-Behra, A.-C., Drobecq, H., Tourret, M., Dubreuil, L., Behra-Miellet, J., 2014. Anti-stress proteins produced by *Bacteroides thetaiotaomicron* after nutrient starvation. Anaerobe 28, 18–23. https://doi.org/10.1016/j.anaerobe.2014.04.008
Leclerc, H., Moreau, A., 2002. Microbiological safety of natural mineral water. FEMS Microbiol. Rev. 26, 207–222. https://doi.org/10.1111/j.1574-6976.2002.tb00611.x
Loper, J.E., Hassan, K.A., Mavrodi, D.V., Ii, E.W.D., Lim, C.K., Shaffer, B.T., Elbourne, L.D.H., Stockwell, V.O., Hartney, S.L., Breakwell, K., Henkels, M.D., Tetu, S.G., Rangel, L.I., Kidarsa, T.A., Wilson, N.L., Mortel, J.E. van de, Song, C., Blumhagen, R., Radune, D., Hostetler, J.B., Brinkac, L.M., Durkin, A.S., Kluepfel, D.A., Wechter, W.P., Anderson, A.J., Kim, Y.C., Iii, L.S.P., Pierson, E.A., Lindow, S.E., Kobayashi, D.Y., Raaijmakers, J.M., Weller, D.M., Thomashow, L.S., Allen, A.E., Paulsen, I.T., 2012. Comparative genomics of plant-associated *Pseudomonas* spp.: insights into diversity and inheritance of traits involved in multitrophic interactions. PLOS Genet. 8, e1002784. https://doi.org/10.1371/journal.pgen.1002784
Manaia, C.M., Nunes, O.C., Morais, P.V., da Costa, M.S., 1990. Heterotrophic plate counts and the isolation of bacteria from mineral waters on selective and enrichment media. J. Appl. Bacteriol. 69, 871–876. https://doi.org/10.1111/j.1365-2672.1990.tb01586.x
Noguera-Mazon, V., Krimm, I., Walker, O., Lancelin, J.-M., 2006. Protein-protein interactions within peroxiredoxin systems. Photosynth. Res. 89, 277–290. https://doi.org/10.1007/s11120-006-9106-4
Richter, M., Rosselló-Móra, R., Oliver Glöckner, F., Peplies, J., 2016. JSpeciesWS: a web server for prokaryotic species circumscription based on pairwise genome comparison. Bioinforma. Oxf. Engl. 32, 929–931. https://doi.org/10.1093/bioinformatics/btv681
Rosen, R., Becher, D., Büttner, K., Biran, D., Hecker, M., Ron, E.Z., 2004. Highly phosphorylated bacterial proteins. Proteomics Weinh. Print 4, 3068–3077. https://doi.org/10.1002/pmic.200400890
Schönfeld, H.J., Schmidt, D., Schröder, H., Bukau, B., 1995. The DnaK chaperone system of

*Escherichia coli*: quaternary structures and interactions of the DnaK and GrpE components. J. Biol. Chem. 270, 2183–2189. https://doi.org/10.1074/jbc.270.5.2183
Shevchenko, A., Wilm, M., Vorm, O., Mann, M., 1996. Mass spectrometric sequencing of proteins from silver-strained polyacrylamide gels. Anal. Chem. 68, 850–858. https://doi.org/10.1021/ac950914h
Surai, K., Surai, P., Speake, B., Sparks, N., 2004. Antioxidant-prooxidant balance in the intestine: Food for thought. 2. Antioxidants. Curr. Top. Nutraceutical Res. 2, 27–46.
Teeling, H., Meyerdierks, A., Bauer, M., Amann, R., Glöckner, F.O., 2004. Application of tetranucleotide frequencies for the assignment of genomic fragments. Environ. Microbiol. 6, 938–947. https://doi.org/10.1111/j.1462-2920.2004.00624.x
Turner, S., Pryer, K.M., Miao, V.P., Palmer, J.D., 1999. Investigating deep phylogenetic relationships among cyanobacteria and plastids by small subunit rRNA sequence analysis. J. Eukaryot. Microbiol. 46, 327–338. https://doi.org/10.1111/j.1550-7408.1999.tb04612.x
Vachee, A., Vincent, P., Struijk, C. b., Mossel, D. a. a., Leclerc, H., 1997. A study of the fate of the autochtonous bacterial flora of still mineral waters by analysis of restriction fragment length polymorphism of genes coding for rRNA. Syst. Appl. Microbiol. 20, 492–503. https://doi.org/10.1016/S0723-2020(97)80018-5
Wood, D.E., Salzberg, S.L., 2014. Kraken: ultrafast metagenomic sequence classification using exact alignments. Genome Biol. 15, R46. https://doi.org/10.1186/gb-2014-15-3-r46
Wu, B., Wawrzynow, A., Zylicz, M., Georgopoulos, C., 1996. Structure-function analysis of the *Escherichia coli* GrpE heat shock protein. EMBO J. 15, 4806–4816.
Yang, X., Song, J., Yan, L.-J., 2019. Chronic inhibition of mitochondrial dihydrolipoamide dehydrogenase (DLDH) as an approach to managing diabetic oxidative stress. Antioxid. Basel Switz. 8, 32. https://doi.org/10.3390/antiox8020032
Zylicz, M., Ang, D., Georgopoulos, C., 1987. The grpE protein of *Escherichia coli*. Purification and properties. J. Biol. Chem. 262, 17437–17442.

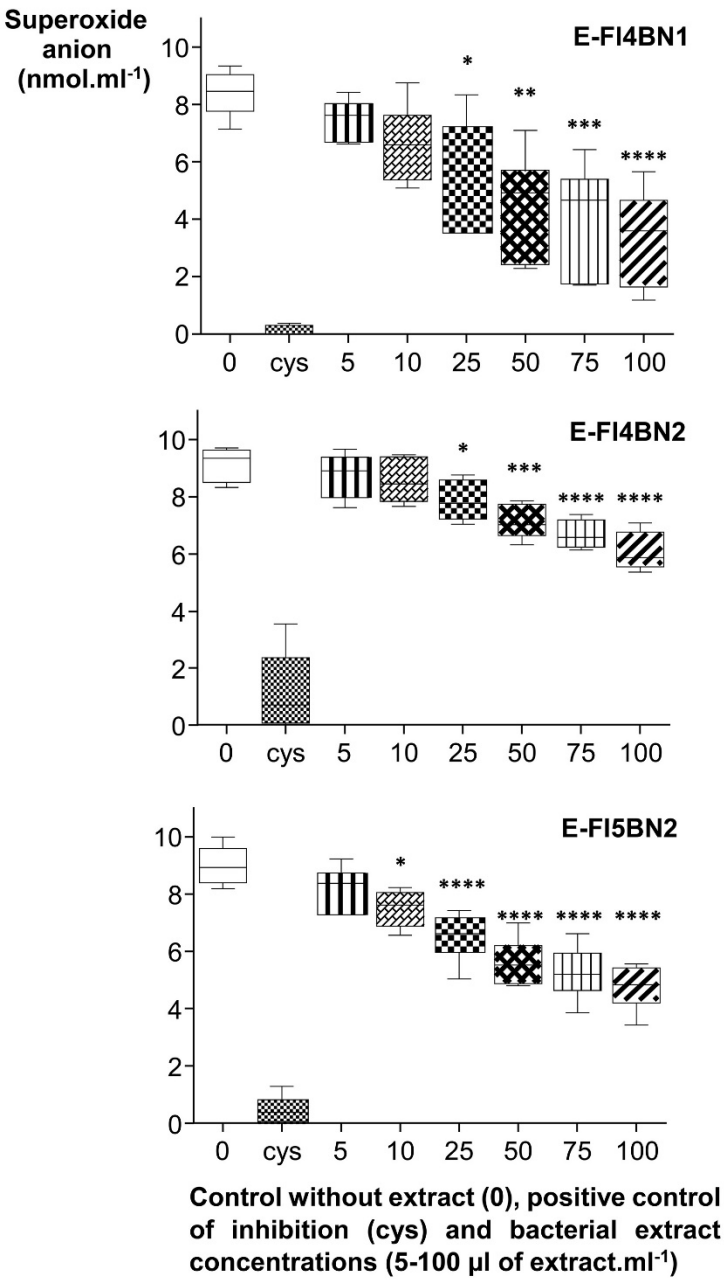


**Fig. 1**. *In vitro* superoxide anion inhibition by the bacterial extracts at increasing concentrations. The effects on $O_2^{\cdot-}$ of 0 to 100 µl of extracts per ml were compared to that of the controls non-containing any extract (0). E-Fl4BN1, E-Fl4BN2 and E-Fl5BN2 are the three bacterial extracts tested. Statistical analysis of the data was performed on 6 independent experiments using ANOVA (overall Fisher's test at the $p = 0.05$ level and Tukeys's multiple a posteriori comparison test with GraphPad Prism software, * $p < 0.05$, ** $p < 0.01$, *** $p < 0.001$, **** $p < 0.0001$). Results are presented as box-plots where the extremities of the lowest and the highest bars represent the 10th and 90th percentiles of percentages for each extract concentration. The 25th, 50th and 75th percentiles correspond to the inferior, interior and superior horizontal bars of the boxes constructed for each of the extract concentrations.

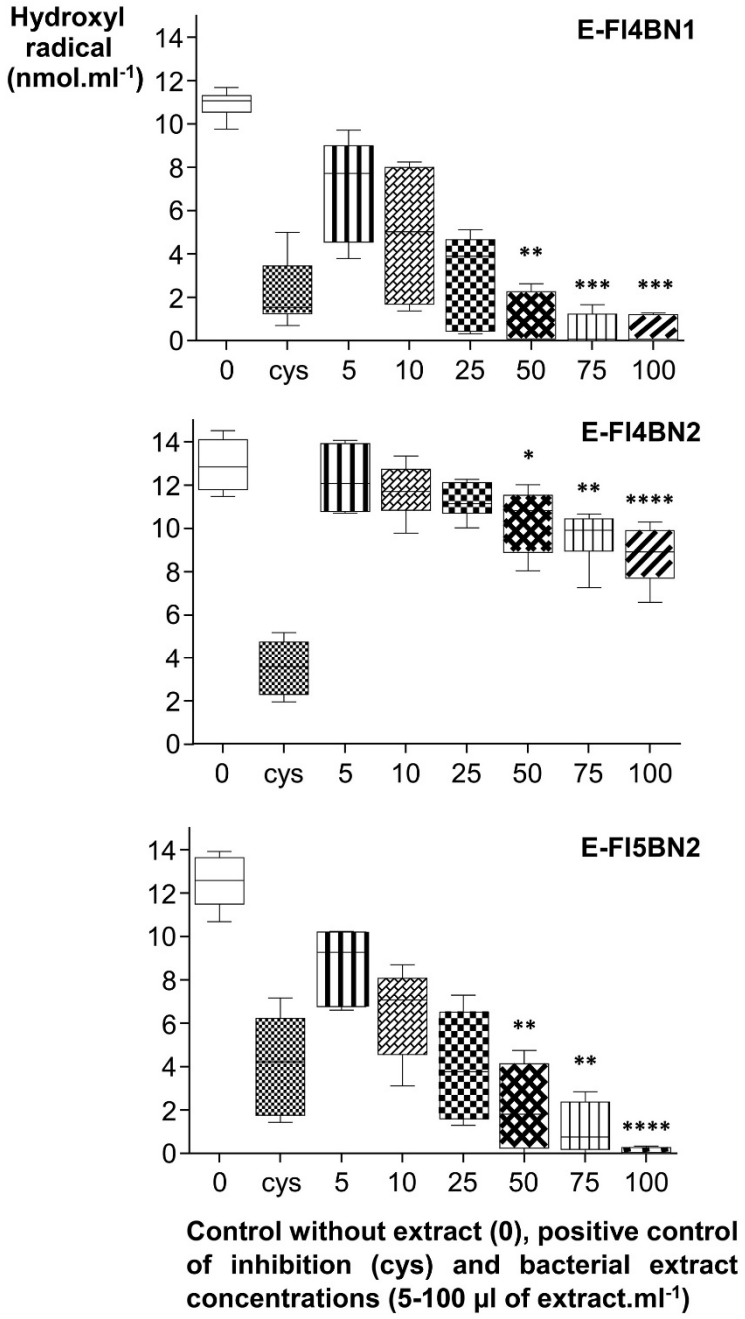


**Fig. 2.** *In vitro* hydroxyl radical inhibition by the bacterial extracts at increasing concentrations. The effects on $HO^{\cdot}$ of 0 to 100 µl of extracts per ml were compared to that of the controls non-containing any extract (0). E-Fl4BN1, E-Fl4BN2 and E-Fl5BN2 are the three bacterial extracts tested. Statistical analysis of the data was performed on 6 independent experiments using the Kruskal Wallis test at the $p = 0.05$ level followed by the Dunn's multiple comparison test to analyze the effects of both E-Fl4BN1 and E-Fl5BN2. ANOVA could be used to analyze the effects of E-Fl4BN2 (overall Fisher's test at the $p = 0.05$ level and Tukeys's multiple *a posteriori* comparison test with GraphPad Prism software. * $p < 0.05$, ** $p < 0.01$, *** $p < 0.001$, **** $p < 0.0001$. Results were presented as box-plots where the extremities of the lowest and the highest bars represent the 10th and 90th percentiles of percentages for each extract concentration. The 25th, 50th and 75th percentiles correspond to the inferior, interior and superior horizontal bars of the boxes constructed for each of the extract concentrations.

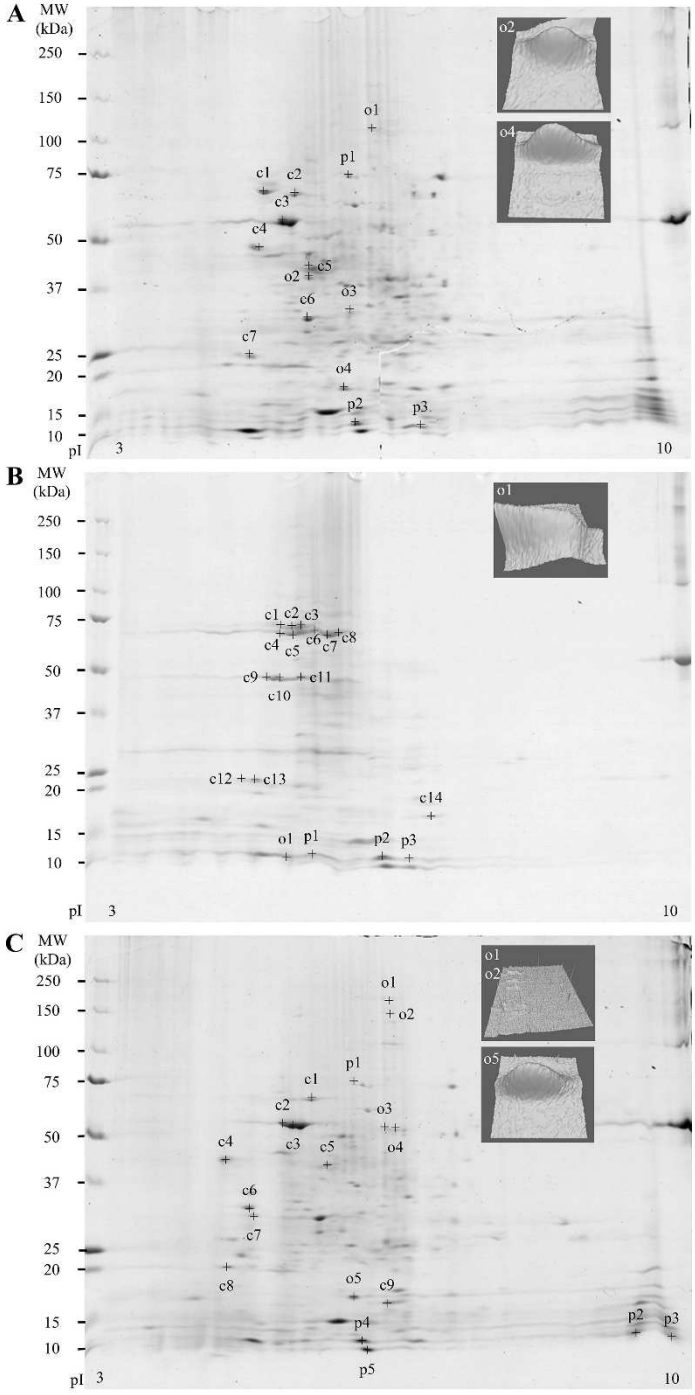


| | Identified proteins | Numbering in gel | MS | MS/MS |
|---|---|---|---|---|
| Proteins counteracting oxidative stress and/or ensuring redox balance | Dihydrolipoyl dehydrogenase | o1 | | x |
| | Peroxiredoxin | o2 | | x |
| | Ketol-acid reductoisomerase (NADP(+)) | o3 | x | |
| | Superoxide dismutase [Fe] | o4 | x | |
| Chaperonin proteins | Chaperone protein DnaK | c1 | | x |
| | Chaperone protein HtpG | c2 | x | x |
| | 60 kDa chaperonin | c3 | | x |
| | Trigger factor | c4 | x | x |
| | Chaperone SurA | c5 | x | x |
| | 60 kDa chaperonin | c6 | | x |
| | Nucleotide exchange factor GrpE | c7 | x | |
| Other proteins involved in stress response | Tail-specific protease | p1 | | x |
| | Cold shock protein CapB | p2 | x | |
| | Cold-shock protein | p3 | | x |

| | Identified proteins | Numbering in gel | MS | MS/MS |
|---|---|---|---|---|
| Proteins counteracting oxidative stress and/or ensuring redox balance | Glutaredoxin | o1 | | x |
| Chaperonin proteins | Chaperone protein DnaK | c1 | x | x |
| | Chaperone protein DnaK | c2 | x | x |
| | Chaperone protein DnaK | c3 | x | x |
| | Chaperone protein DnaK | c4 | x | x |
| | Chaperone protein DnaK | c5 | x | x |
| | Chaperone protein DnaK | c6 | x | x |
| | Molecular chaperone HtpG | c7 | x | |
| | Chaperone protein HtpG | c8 | | x |
| | Trigger factor | c9 | x | x |
| | Trigger factor | c10 | x | x |
| | Trigger factor | c11 | x | x |
| | Protein GrpE | c12 | | x |
| | Protein GrpE | c13 | | x |
| | Peptidyl-prolyl cis-trans isomerase | c14 | | x |
| Other proteins involved in stress response | Cold-shock protein CapB | p1 | | x |
| | Cold-shock protein CapB | p2 | x | x |
| | Cold-shock protein CapB | p3 | | x |

| | Identified proteins | Numbering in gel | MS | MS/MS |
|---|---|---|---|---|
| Proteins counteracting oxidative stress and/or ensuring redox balance | Dihydrolipoyl dehydrogenase | o1 | | x |
| | Dihydrolipoyl dehydrogenase | o2 | | x |
| | Dihydrolipoyl dehydrogenase | o3 | x | x |
| | Dihydrolipoyl dehydrogenase | o4 | x | |
| | Superoxide dismutase | o5 | x | x |
| Chaperonin proteins | Chaperone protein HtpG | c1 | | x |
| | 60 kDa chaperonin | c2 | x | x |
| | 60 kDa chaperonin chaperonin GroEL | c3 | | x |
| | Trigger factor | c4 | x | |
| | Molecular chaperone SurA | c5 | x | |
| | Chaperone protein DnaK | c6 | | x |
| | Chaperone protein DnaK | c7 | | x |
| | Peptidyl-prolyl cis-trans isomerase | c8 | | x |
| | Peptidyl-prolyl cis-trans isomerase | c9 | | x |
| Other proteins involved in stress response | C-terminal processing peptidase-1, Serine peptidase | p1 | x | |
| | DNA-binding protein HU, beta subunit | p2 | | x |
| | DNA-binding protein HU, beta subunit | p3 | | x |
| | Cold-shock protein | p4 | x | x |
| | Cold-shock protein | p5 | | x |

**Fig. 3.** Protein profiles of the extract proteins from Fl4BN1 (A), Fl4BN2 (B) and Fl5BN2 (C). They were obtained after 2D-PAGE under non-denaturing conditions and Coomassie blue staining. Isoelectrofocalisation was performed using precast immobilized pH 3-10 gradient ReadyStrip® (17 cm Bio-Rad). SDS-PAGE native gels were obtained with 4-20% acrylamide gradient (only 0.1% SDS without protein reduction/alkylation). Stress proteins were identified by mass spectrometry (MS) and/or MS/MS through two search algorithms (PEAKS and MASCOT) and two databases (NCBI and SwissProt). The crosses in the table indicate by what techniques the proteins were identified. (o) Proteins counteracting oxidative stress and/or ensuring redox balance; (c) chaperonin proteins; (p) other proteins involved in stress response. (MW) Molecular weight standards expressed in kilo Daltons (kDa). (pI) Isoelectric points.

**1. Phenotypic identification of strains:**

- API® 20 NE
- API® 50 CH

↓

First identification:
*Pseudomonas fluorescens*

**2. Genomic assays:**

- 16S RNA: genus confirmation
  → *Pseudomonas*
- Draft genomes
  → Tetra correlation search
  → Average nucleotide identity

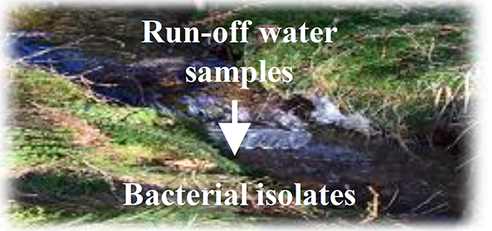


**Extraction**
**Incubation in sterile distilled water (20 h; + 4°C)**

↓

Centrifugation → supernatants
= **bacterial extracts**
**(cell-free extracts)**

**3. Pharmacological *in vitro* assays**

- Effects of the bacterial extracts on superoxide anion
- Effects of the bacterial extracts on hydroxyl radical

↓

Discrepancies between the anti-oxidative effects of the three strains

**4. Proteomic assays:**

2D-PAGE, MS and MS/MS
→ stress proteins:

- proteins counteracting oxidative stress and/or ensuring redox balance;
- chaperonin proteins;
- other proteins involved in stress response.